International Journal of Artificial Intelligence,
ISSN 0974-0635; Int. J. Artif. Intell.
Spring (March) 2013 , Volume 10, Number S13

Control Architecture of an Autonomous Material Handling Vehicle

Augie Widyotriatmo[1], **Anugrah K. Pamosoaji**[2] and **Keum-Shik Hong**[3]

[1] Instrumentation and Control Research Group, Faculty of Industrial Technology, Bandung Institute of Technology; Ganesha 10, Bandung 40135, Indonesia;
Email: augie@tf.itb.ac.id

[2] School of Mechanical Engineering, Pusan National University; 30 Jangjeon-dong Geumjeong-gu, Busan 609-735, Korea;
Email: nugie161@pusan.ac.kr

[3] Department of Cogno-Mechatronics Engineering and School of Mechanical Engineering, Pusan National University; 30 Jangjeon-dong Geumjeong-gu, Busan 609-735, Korea;
Email: kshong@pusan.ac.kr

ABSTRACT

In this paper, a control architecture that integrates path planning and motion control of an autonomous material handling vehicle is proposed. The three-layer architecture (deliberative, sequencing, and reflexive layers) is adopted. The deliberative layer plans a series of control actions for accomplishing tasks, the sequencing layer regulates the sequence of control modules and supervises the change of plan, and the reflexive layer collects sensory data and controls a specific motion. The control algorithms, which are derived considering sensor, environment, and kinematic constraints of the autonomous vehicle, assure the robustness against uncertainties as well as the safety during the motion. A finite state machine (FSM) that regulates the excecution of the planning and various control algorithms is proposed. The experimental results of a forklift transporting a pallet from an initial to a desired goal configuration demonstrate the effectiveness of the proposed control architecture.

Keywords: Autonomous vehicle, forklift, control architecture, path planning, motion control.

Mathematics Subject Classification: 68T40, 93C85

Computing Classification System: I.2.9

1. INTRODUCTION

Robotics research has been increased significantly in recent years. The applications of robotics include material handling vehicles (Tamba, Hong, and Hong, 2009; Widyotriatmo, Hong, and Prayudhi, 2010), robot manipulator (Hassanein, Anavatti, and Ray, 2011), multi agent system for hose transportation (Fernandez-Gauna et al., 2011), and others. The research subjects include localization and vision systems (Takemura and Ishii, 2011; Bui and Hong, 2012), obstacle avoidance strategy (Bui and Hong, 2010), control design (Nguyen, Hong, and Park, 2010; Turnip, Park, and Hong, 2010; Haidegger et al., 2011; Joelianto and Wiranto, 2011), planning (LaValle, 2006), and the integration of the components and algorithms (Hong, Tamba, and Song, 2008). This paper discusses the architecture that organizes the planning, the control modules, and the integration of planning and control for an autonomous forklift that has two caster wheels in the front and one drivable-and-steerable (driving) wheel in the rear.

The objective of an autonomous material handling vehicle is to transport materials from an initial to a destination. A high speed movement, accident preventive motion, failure recovery action, and high precision motion are demanded in the design of the autonomous material handling vehicle. To handle such multiple objectives, different control modules need to be developed. Control architectures of mobile robots have been developed in many approaches (Arkin, 1998). A purely reactive behavior has been proposed in (Brooks, 1986). However, the purely reactive scheme does not perform well when performing complex tasks. In (Arkin, 1992; Gerkey and Mataric, 2002), a behavior based control architecture that has a hierarchical system consisting of a mission planner, a plan sequencer, and a reactive system was proposed. In (Oreback and Christensen, 2003), three-layer architecture (deliberative, sequencing, and reflexive layers) was proposed. The deliberative layer plans the tasks given to the vehicle, the sequencing layer regulates action modules in the reflexive layer, and the reflexive layer consists of resources (that collect data from various sensors), action modules (that control a vehicle to perform various motions), and motor control modules (that regulate the motors in the fashion that the desired commands given by an action module are followed).

Path planning algorithms generate a free collision path from an initial to a goal configuration based upon a map information that provides sets of free-space and of obstacles (LaValle, 2006). Various methods of path planning method are as follows: the grid-based search method assumes that each configuration is identified by a grid point, and search algorithms are used to find a path from the start to the goal avoiding obstacles; the cell decomposition method divides the map into polygonal region of free space and obstacles; and sampling based algorithms represent a free space with a roadmap of sampled configurations.

The control algorithms for a forklift become difficult since the forklift is a nonholonomic system (i.e., a system with nonholonomic constraints). In (Brockett, 1983), it was shown that there is no continuously differentiable time-invariant control law that stabilizes a nonholonomic system asymptotically. Two control strategies for nonholonomic systems are found in the literature: open loop and closed loop strategies. In open loop strategies (Murray and Sastry, 1993; Widyotriatmo, Hong, and Hong, 2009), the control signals are calculated off-line using the information of the initial and the goal configurations. Using this strategy, the vehicle may not reach the goal configuration due to disturbances, modeling errors, and sensor uncertainties. In closed loop strategies, time-varying controls (Samson, 1995; Tamba, Hong, & Hong, 2009) and discontinuous controls (Astolfi, 1996; Widyotriatmo and Hong, 2012) have been proposed. The control signals are computed online based on the current and goal configurations. A closed loop control can potentially compensate the uncertainties. In (Widyotriatmo and Hong, 2011), a collision avoidance method which drives a forklift from an initial to a goal configuration while avoiding collisions was investigated. In (Belta, Isler, & Pappas, 2005; Lindemann & LaValle, 2009; Conner, Choset, and Rizzi, 2009), integration methods for planning and control of robots were investigated. The planning was based on cell decomposition method, and vector field algorithms for controlling the vehicle the was proposed. However, the methods assume static obstacles, and the position of all of the obstacles are known

In this paper, the algorithms for the material handling task of the autonomous forklift are elaborated as follows. A planning algorithm generates way-points from an initial configuration to a desired final configuration based upon the map. The path planning algorithm is developed by two steps: A set of points that include allowable position of the vehicle is determined from a given map; and the A* algorithm in (LaValle, 2006) is used to obtain the shortest path from an initial to a goal. The control algorithms includes path tracking algorithm to steer the forklift following a desired path, configuration control to pick up or unload a pallet at a specified location, and collision avoidance algorithm to prevent collision with dynamic and unmodeled obstacles. A FSM algorithm that integrates path planning and control algorithms is proposed. It regulates the excecution of planing and motion control algorithms in such away that the vehicle can accomplish the material transportation.

The contributions of the paper are as follows. First, the control architecture of the autonomous material-handling vehicle is discussed. Second, the control modules required for the individual material handling vehicles are investigated. Third, the reflexive layer structure, in which the control modules are implemented, is elucidated. Fourth, the integration of path planning and control algorithms for the material handling forklift is proposed. Fifth, the experimental results of the proposed method are presented.

The paper is organized as follows. Section 2 describes the hardware configuration of the autonomous forklift. Section 3 presents the software architecture of the autonomous forklift. Section 4 presents the autonomous navigation controls. Section 5 demonstrates the experimental results of a forklift transporting a pallet from an initial to a desired location. Section 6 draws conclusions.

2. HARDWARE CONFIGURATION

The hardware configuration of the autonomous vehicle is shown in Figure 1. Two AC motors drive and steer the rear wheel and one AC motor drives a ball screw for the fork motion. Each forklift is equipped with a laser-based localization sensor SICK NAV200 that measures its position and orientation in a predefined global coordinate which is based upon known positions of reflectors. A laser range finder (LRF) Hokuyo URG-04LX (range 4 m) provides the measurement of the distance and the angle to obstacles. A webcam with a FOV of 50^{o} (or 0.28π rad) is used to identify and measure the configuration of a pallet. A wireless router is used for communication with the central computer. The front and rear bumpers and emergency buttons are provided for safety.

In Figure 2, the hardware configuration of a forklift is shown including two controllers: an embedded PC and a programmable logic controller (PLC). The PC receives the vehicle’s current configuration from the NAV200, the distance and angle of obstacles from the LRF, the vision information from the webcam, and a task from the central computer from the wireless router. It also provides control commands (linear velocity and steering angle of the driving wheel and height position of the fork) to the PLC.

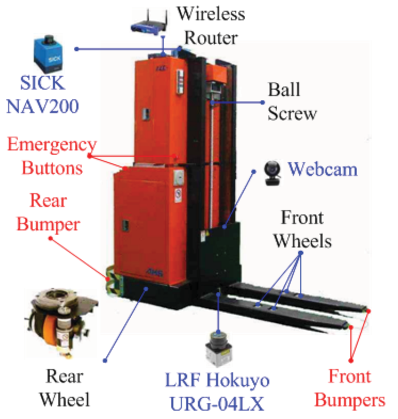

Figure 1. The autonomous forklift.

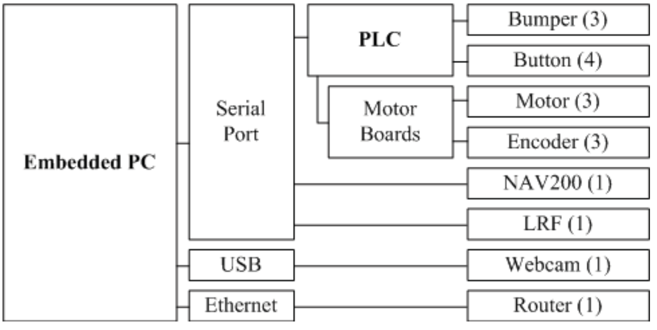

Figure 2. Hardware configuration of the autonomous forklift.

The PLC controls three motors (driving, steering, and fork) by utilizing feedbacks from their individual encoders such that the driving wheel and the fork follow the desired commands. It also receives the signals from the three bumpers (two bumpers in the front and one bumper in the rear) and four emergency buttons. The bumpers and the emergency buttons switches off the control signals to the motor driver if they are activated. The PC communicates with the PLC, NAV200, and LRF via RS232 (serial port), with the webcam via USB, and with the wireless router via Ethernet.

3. CONTROL ARCHITECTURE

3.1. Three-layer architecture

Figure 3 depicts the three-layer (i.e., deliberative, sequencing, and reflexive) architecture. After a vehicle is assigned to move a pallet to its destination, the deliberative layer plans a series of actions: pick up the pallet using the information from vision system, follow a path/via-point directing to the goal area, avoid collisions during movement, reach the goal configuration, and unload the pallet at the desired configuration. The deliberative layer then enters a monitoring mode to begin checking the results. The sequencing layer regulates a specific set of actions and also monitors the conditions of every event. The sequencing layer will terminate an action, or replace them with a new action when a monitoring event is triggered, when a timeout occurs, or when a new message is received from the deliberative layer indicating a change of plan. The reflexive layer consists of resource, action, and motor control. A resource represents a shared memory of sensor data. The data is utilized by the action modules, the sequencing, and the deliberative layers. An action is a module to perform a situated motion. In material handling vehicles systems, action modules include the following: configuration control is to drive the vehicle from an initial to a specified goal configuration; path tracking control is to move the vehicle following a particular path; and collision avoidance is to steer the vehicle reaching a goal/sub-goal configuration while avoiding obstacles and other vehicles. Motor control receives the desired control commands, converts them into proper signals, and controls the motors such that the desired control commands are achieved.

3.2. Reflexive layer

Block diagram in Figure 4 shows the detail of the reflexive layer structure that is decomposed into two loops: outer loop and inner loop. The outer loop, programmed in C++ on the embedded industrial PC, generates three desired commands: the linear velocity (v_d), the steering angle (δ_d) of the driving wheel, and the fork height position (z_d). These commands are updated upon the feedbacks from the sensors: NAV200 provides position and orientation measurement (x, y, θ) with 10 Hz-frequency; LRF provides distance and angle of the *i*-th obstacle (ρ_i, θ_i); the webcam provides the configuration of the pallet (x_g, y_g, θ_g, z_g); and the encoders provides the angular positions of the driving, steering, and fork motors (φ_r, φ_δ, φ_z). The inner loop, implemented in the PLC, generates three control signals (voltages u_v, u_δ, and u_z) to control the three AC motors (driving, steering, and fork) in the fashion that the driving wheel and the fork follow the desired commands. The three voltages are calculated from the desired commands and the encoders' feedback with the frequency of 100 Hz.

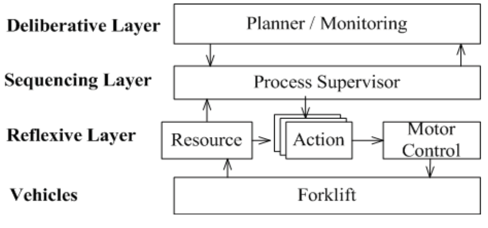

Figure 3. The three (deliberative, sequencing, and reflexive) layer architecture.

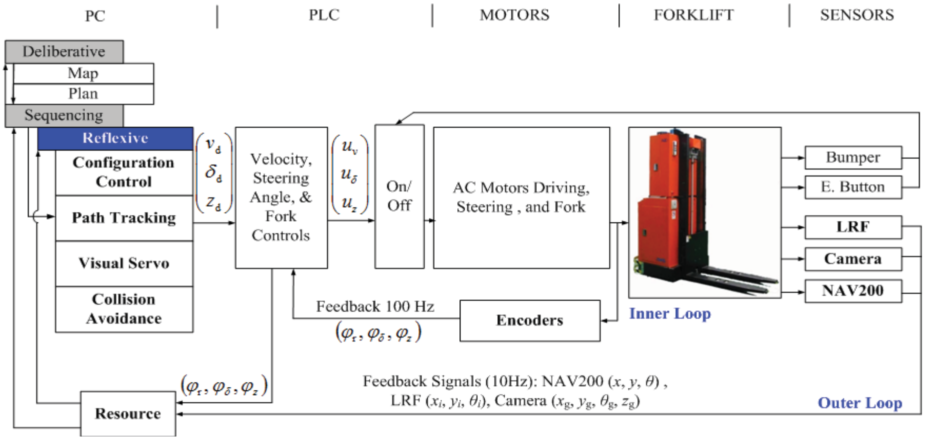

Figure 4. Block diagram of the reflexive layer.

4. PLANNING AND CONTROL ALGORITHMS

4.1. Global path planning

For the global planning strategy, via-points that provide a set of free space in a given workspace are assigned. The via points can be generated using any path planning algorithm such as voronoi diagram, cell decomposition, or sampling-based algorithm. In this paper, the via points are generated manually since the static information of the map is known. The assignment of via points in the given map is shown in Figure 5. To navigate the vehicles, paths are generated through the via-points from the initial to the desired configurations. The sequence of the via-points for the individual vehicles is computed in a discrete fashion using search algorithms. In this paper, the A* algorithm (LaValle, 2006) is utilized in generating the path through via points from an initial to a goal configuration.

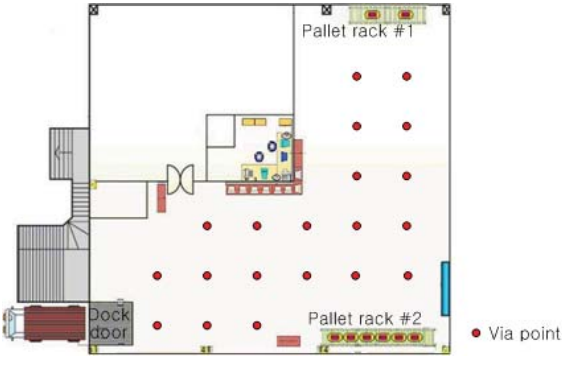

Figure 5. Via points assigned in the given map.

4.2. Forklift model

In Figure 6, $O\text{-}\hat{i}\hat{j}$ represents the global coordinate frame that is fixed in the workspace. $O_b\text{-}\hat{i}_b\hat{j}_b$ denotes the body coordinate frame attached to the vehicle, O_b is the mid-point of the two front wheels to which all the motions of the vehicle are generated, l denotes the distance between the center of the rear wheel and the reference point O_b. The configuration of the vehicle is specified by position (x, y) which is the coordinates of the reference point O_b and orientation θ which is the angle from the $\hat{i}$ -axis to the $\hat{i}_b$ -axis. The velocity v and steering angle δ are the rear wheel's linear velocity and steering angle from the $\hat{i}_b$-axis, respectively. The equations of motion of the forklift are as follows (Widyotriatmo and Hong, 2012):

$$\dot{x} = v\cos\theta\cos\delta\,, \tag{1}$$

$$\dot{y} = v\sin\theta\cos\delta\,, \tag{2}$$

$$\dot{\theta} = -(v/l)\sin\delta\,, \tag{3}$$

$$m_1\dot{v} + c_1 v + r_r f_v = \tau_v\,, \tag{4}$$

$$I_\delta\ddot{\delta} + f_\delta = \tau_\delta\,, \tag{5}$$

where

$$m_1 = r_r\left((m + I_f)\cos^2\delta + \left(I_b/l^2\right)\sin^2\delta + I_r\right), \tag{6}$$

$$c_1 = r_r\left(\left(I_b/l^2\right) - \left(I_f/r_f^2\right) - m\right)\cos\delta\sin\delta\dot{\delta}\,, \tag{7}$$

m is the vehicle mass, I_b is the mass moment of inertia of the vehicle with respect to O_b, I_δ is that of the rear wheel around the normal axis of the flat surface, I_f and I_r be the mass moments of inertia of the front and rear wheels around their individual rolling axes, τ_v and τ_δ are the torque inputs vector to the driving and steering motors, respectively, f_v and f_δ are the surface frictions of the rear wheel in the rolling and steering directions, respectively.

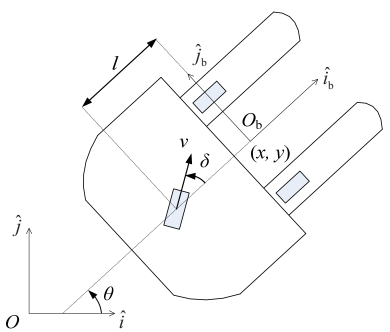

Figure 6. The forklift model.

The equations of motion of the forklift are consisted of two parts: Kinematic equations (1)-(3) describe the configuration motion of the vehicle where the control commands are the linear velocity and the steering angle of the driving wheel, and dynamic equations (4)-(5) provide the relationship between the dynamics of the vehicle and the torques of the two AC motors (driving and steering). The two parts of equations express the system in two (outer and inner) loops as described in Figure 4. The control problem of the vehicle is solved in two stages: the desired input commands (linear velocity and steering angle of the driving wheel) are designed based upon the kinematic equations, and the voltage inputs supplied to the motors (driving and steering) are computed based upon the dynamic equations. In this dissertation, a conventional PD control algorithm is implemented in the AC motor control. In (Widyotriatmo and Hong, 2012), it was shown that the linear velocity v and the steering angle δ tracks the desired commands v_{d} and δ_{d} with tracking errors $\tilde{v} = v - v_{\mathrm{d}}$ and $\tilde{\delta} = \delta - \delta_{\mathrm{d}}$ caused by the frictions and transient responses. As the load of the forklift m increases, the response converge slowly, and therefore, the two tracking errors ($\tilde{v}$ and $\tilde{\delta}$) also increase. It is assumed that the load variation during motions is very small and by using the fixed gains of PD control, the linear velocity v and steering angle δ can track their desired values v_{d} and δ_{d} with small bounded tracking errors $|\tilde{v}| \le \bar{\tilde{v}}$ and $|\tilde{\delta}| \le \bar{\tilde{\delta}}$, where $\bar{\tilde{v}}$ and $\bar{\tilde{\delta}}$ are their bounds.

4.4. Configuration controls

In this section, the configuration (position and orientation) control (Widyotriatmo & Hong, 2011) that drives the vehicle from an initial to a goal configuration and the path tracking control that steers the vehicle to follow a determined path are developed. Let $\tilde{x} = x_{\mathrm{g}} - x$, $\tilde{y} = y_{\mathrm{g}} - y$, and $\tilde{\theta} = \theta_{\mathrm{g}} - \theta$ be the configuration errors between the current and goal configurations. Three navigation variables are introduced: $\rho = \sqrt{\tilde{x}^2 + \tilde{y}^2}$ is the distance error, and $\alpha = \arctan 2(\tilde{y}, \tilde{x}) - \theta$ and $\phi = \theta_{\mathrm{g}} - \arctan 2(\tilde{y}, \tilde{x})$ are the split portions of the orientation error (i.e., $\tilde{\theta} = \alpha + \phi$), in which α is the portion from the vehicle's moving direction to the goal point direction and ϕ is the remaining error at the goal frame. The kinematic equations (1)-(3) using the introduced navigation variables become

$$\dot{\rho} = -v \cos\alpha \cos\delta\,, \tag{8}$$

$$\dot{\alpha} = (v/\rho)\sin\alpha \cos\delta + (v/l)\sin\delta\,, \tag{9}$$

$$\dot{\phi} = -(v/\rho)\sin\alpha \cos\delta\,. \tag{10}$$

If the vehicle achieves its goal configuration, both ρ and $\tilde{\theta}$ ($\alpha + \phi$) become zero. Let the polar coordinate system comprising ρ and $\tilde{\theta}$ be the error space. The control problem of moving a vehicle from an initial configuration to a goal configuration becomes the asymptotic stabilization problem from an arbitrary point in the error space to its origin.

The movements of the vehicle from an initial configuration to a goal configuration are considered in two ways: forward and backward. Whenever a goal point is in front of the vehicle, the forward movement is chosen. Conversely, the backward movement is chosen when a goal point is behind the vehicle. Consider the system (8)-(10). The control law with the goal points in front of the vehicle is given as follows:

$$v = \sqrt{\left(k_{v,1}\rho\cos\alpha\right)^2 + l^2\left(k_{v,2}\sin\alpha - \left(k_{v,2} - k_{v,1}\cos\alpha\right)\phi\right)^2}\ , \tag{11}$$

$$\delta = -\arctan\left(l\left(\frac{k_{v,2}\sin\alpha - \left(k_{v,2} - k_{v,1}\cos\alpha\right)\phi}{k_{v,1}\rho\cos\alpha} \right)\right), \tag{12}$$

where $k_{v,1}$ and $k_{v,2}$ are positive constants with $k_{v,2} > 2k_{v,1} > 0$. Then, the origin (ρ , α , ϕ) = (0, 0, 0) is uniformly asymptotically stable. The control law with the goal points behind the vehicle is given as follows:

$$v = -\sqrt{\left(k_{v,1}\rho\cos\alpha\right)^2 + l^2\left(k_{v,2}\sin\alpha + \left(k_{v,2} + k_{v,1}\cos\alpha\right)(\phi - \pi)\right)^2}\ , \tag{13}$$

$$\delta = -\arctan\left(l\left(\frac{k_{v,2}\sin\alpha + \left(k_{v,2} + k_{v,1}\cos\alpha\right)(\phi - \pi)}{k_{v,1}\rho\cos\alpha} \right)\right). \tag{14}$$

Then, (ρ , α , ϕ) = (0, π , π) is uniformly asymptotically stable. The proofs of the control laws (11)-(14) can be found in (Widyotriatmo & Hong, 2011). The control law (11)-(12) drives the vehicle from an initial to a goal configuration in forward movement, while the control law (13)-(14) steers the vehicle in backward movement.

4.5. Path tracking control

The path tracking problem is formulated as a configuration control, in which the goal configuration moves along the path *s* with the velocity $\dot{s}$. In order that the vehicle can follow the motion of the goal configuration, the velocity $\dot{s}$ is designed subject to the current-goal configuration errors of the vehicle. The velocity $\dot{s}$ be chosen as

$$\dot{s} = \pm\max(0, v_{\max} - (1/k_q)\sqrt{\rho^2 + \alpha^2 + \phi^2}\,)\ , \tag{15}$$

where $v_{\max}$ is the maximum velocity of the vehicle and k_q is a positive constant. The sign (positive or negative) in (15) assigned the trajectory to be followed in forward or backward movement. Applying (11)-(12) with the velocity of moving goal configuration $\dot{s} = \max(0, v_{\max} - (1/k_q)\sqrt{\rho^2 + \alpha^2 + \phi^2}\,)$, the vehicle follows the assigned trajectory s in forward movement. Conversely, applying (13)-(14) with the velocity of moving goal configuration $\dot{s} = -\max(0, v_{\max} - (1/k_q)\sqrt{\rho^2 + \alpha^2 + \phi^2}\,)$, the vehicle follows the assigned trajectory s in backward movement.

4.6. Collision avoidance

The collision avoidance control for the individual vehicle is derived based upon the navigation function, that is a function in which the negative gradient of the function induces the vehicle to be attracted toward a desired configuration and repelled against obstacles (Widyotriatmo and Hong, 2011). A control law is designed based upon the negated gradient of the navigation function, so that the system is driven from an initial configuration to a goal configuration as the elements in the system avoid collisions. The navigation function is proposed as follows:

$$V=\frac{1}{2}\frac{\rho^2+\phi^2+\alpha^2}{\left((\rho^2+\phi^2+\alpha^2)^{\kappa}+\prod_{i=1}^{n}\gamma_i+\prod_{i=1}^{n}\beta_i^2\right)^{1/\kappa}}, \tag{16}$$

where $\gamma_i(x,y)=\rho_i^2(x,y;x_i,y_i)-(r+r_i)^2$ and $\beta_i=\operatorname{atan2}(y_i-y,\ x_i-x)-\theta$. The navigation function (16) is proposed based upon the fact that a vehicle configuration that is close to and is directed to obstacles should be avoided.

The control law is derived in such away that the time derivative of (16) is negative semi-definite. The control law is (Widyotriatmo and Hong, 2011)

$$v=k_{v,1}(\rho\cos\alpha-\overline{\rho}), \tag{17}$$

$$\delta=-\tan^{-1}\left(\frac{l}{k_{v,1}(\rho\cos\alpha-\overline{\rho})}(k_{v,2}\alpha(1-\overline{\alpha})+\frac{k_{v,1}(k_{v,2}\alpha+\phi)}{k_{v,2}\alpha}(k_{v,1}\cos\alpha-\frac{\overline{\rho}}{\rho})\sin\alpha-\overline{\xi})\right), \tag{18}$$

where

$$\overline{\rho}=\psi'_{\gamma}(z/\kappa)\sum_{i=1}^{n}(\rho_i/\gamma_i)\cos\beta_i\ , \tag{19}$$

$$\overline{\alpha}=\psi'_{\beta}(z/(\kappa k_{\alpha}\alpha))\sum_{i=1}^{n}(1/|\beta_i|), \tag{20}$$

$$\overline{\xi}=\psi'_{\beta}\frac{z}{\kappa k_{\alpha}\alpha}k_{v_{dr}}(k_{\rho}\rho\cos\alpha-\overline{\rho})\sum_{i=1}^{n}\frac{\sin\beta_i}{|\beta_i|\rho_i}, \tag{21}$$

$$\psi'_{\gamma}=\psi_{\gamma}/(\psi_{\gamma}+\psi_{\beta}), \tag{22}$$

$$\psi'_{\beta}=\psi_{\beta}/\psi_{\gamma}+\psi_{\beta}, \tag{23}$$

$$\psi_{\gamma}=(k_{\gamma}\prod_{i=1}^{n}\gamma_i)/(z^{\kappa}+k_{\gamma}\prod_{i=1}^{n}\gamma_i+k_{\beta}\prod_{i=1}^{n}\beta_i^2)^{\frac{1}{\kappa}+1}, \tag{24}$$

$$\psi_{\beta}=(k_{\beta}\prod_{i=1}^{n}\beta_i^2)/(z^{\kappa}+k_{\gamma}\prod_{i=1}^{n}\gamma_i+k_{\beta}\prod_{i=1}^{n}\beta_i^2)^{\frac{1}{\kappa}+1}. \tag{25}$$

Then, the origin (ρ , α , ϕ) = (0, 0, 0) is uniformly asymptotically stable. The proof is found in (Widyotriatmo & Hong, 2011). Using the control law (17) and (18), the forklift achieves a via point or a goal configuration, and the collisions with obstacles and moving objects are avoided.

4.7. Integration of path planning and control

This section describes the integration of the four algorithms: global path planning, configuration control, path tracking controls, and collision avoidance, to move the vehicle from an initial to a goal configuration. The algorithms are excecuted by the FSM that regulates the four algorithms based upon the vehicle conditions (Figure 7). The conditions are described as follows:

- FVP (final via point) is a condition whether the vehicle has or has not reached the final point. FVP = 1 denotes that the final via point is reached, and FVP = 0 denotes that the final via point is not reached.
- VP (via point) is a condition whether the vehicle has or has not reached the next via point. VP = 1 denotes that the next via point is reached, and VP = 0 denotes that the next via point is not reached.
- TO (timeout) is a condition whether the vehicle has or has not passed the timeout given to reach the next point. TO = 1 denotes that the timeout is reached, and TO = 0 denotes that the timeout is not reached.
- OB (obstacles) is a condition whether the vehicle does or does not detect obstacles along its way to the next point. OB = 1 denotes that the vehicle detects obstacles, and OB = 0 denotes that the vehicle does not detect obstacles.

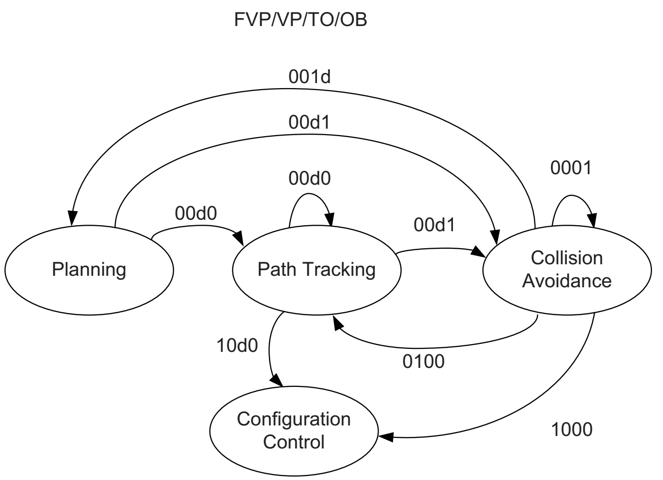

Figure 7. The FSM that regulates the four algorithms to drive the vehicle from the initial to the goal configuration. The events are the following. FVP: final via point, VP: via point, TO: timeout, and OB: obstacles. If the events are met then it is denoted as 1. If not, it is denoted as 0, and d is the don't care condition.

The FSM in Figure 7 is described as follows. From Subsection 4.1, the global planning algorithm produces a set of via points from an initial to a goal configuration. If there is no obstacle along the way to the next via point, the vehicle excecutes the path tracking algorithm. On the other hand, if obstacle exists, the vehicle runs the collision avoidance algorithm. When the vehicle is at the state of collision avoidance, a timer to determine a given timeout is set. If the vehicle has reached the next via point (or the final via point) within the given timeout, the vehicle runs the path tracking (or the configuration control) to go to the next via point. If the given timeout has passed and the next or final via point has not been reached, the planning algorithm is excecuted. Thus, this prevents the vehicle to be trapped in the local minima by following a new planning. When the vehicle has reached the final via point and there is no obstacle along the way to the goal configuration, the algorithm is switched to configuration control. Then, the desired configuration of the vehicle is achieved.

5. EXPERIMENTAL RESULTS

In this section, the performance of the proposed navigation planning and control is investigated. Fig. 8 shows the experiment of the pallet loading from the initial to the pallet location. At the initial position, the forklift calculated a set of via points from the initial to the goal point (pallet position) throuhgh A* algorithm. Then, it detected an obstacle along the way to the next via-point. The collision avoidance module was activated to avoid the obstacle and reach the next via-point. When the forklift reached the final via-point, it excecuted the configuration control to reach the goal position and orientation, and engaged the pallet.

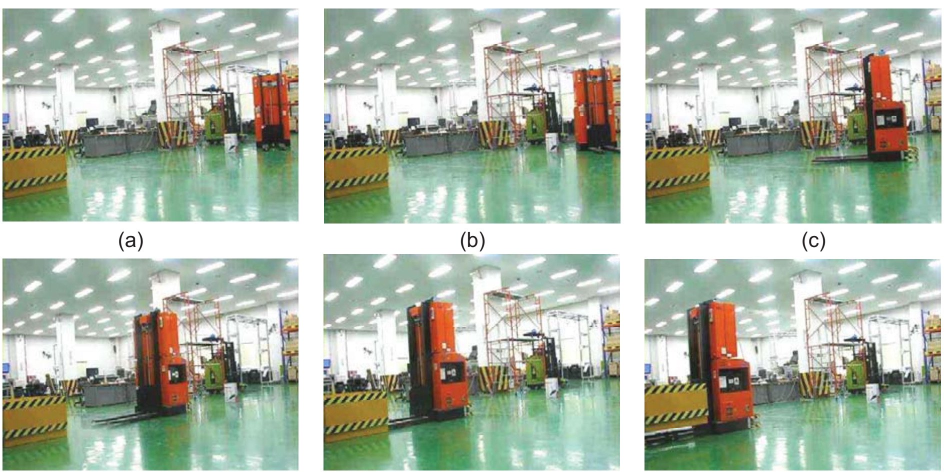

(a) (b) (c)

(d) (e) (f)

Figure 8. The experiment of pallet loading: (a)-(c) the forklift detected obstacle, and performed collision avoidance, (d)-(f) the forklift reached final via point, performed configuration control, and lifted the pallet.

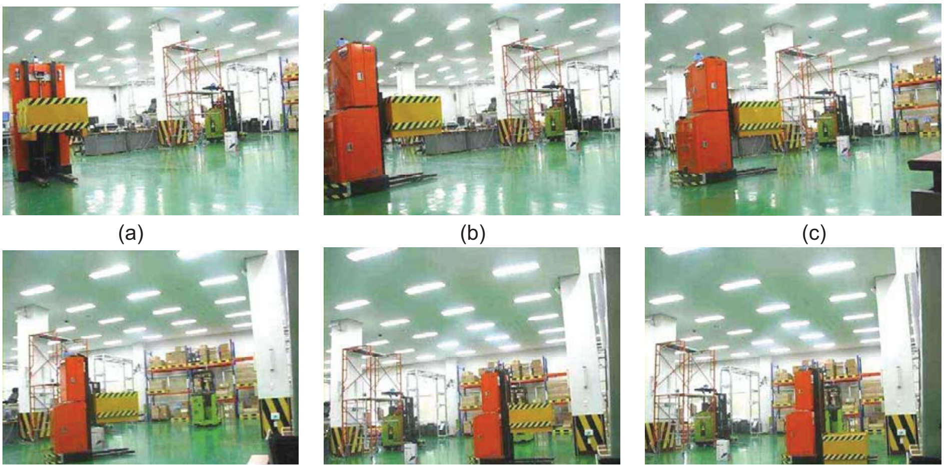

Figure 9. The experiment of pallet unloading: (a)-(d) the forklift tracks the via-points, (e)-(f) the forklift reached the final via point, performed configuration control, and unload the pallet.

Fig. 9 depicts the experiment of the pallet transfer from the pallet location to the destination. The forklift calculated a set of via points from the initial to the goal point (pallet destination) through A* algorithm. Since there is no obstacle along the way to the final via-point, the vehicle performed path tracking control. When the final via point was reached, the configuration control was performed, and the pallet was unload to the destination. In this experiment, the maximum speed of the vehicle was set to 0.8 m/s. The forklift took 2 minutes to accomplish the task. The slow velocity was due to the low rate of the sensors sampling time (i.e., the sampling time of the LRF and the vision processing were 500 ms and that of the NAV200 was 100 ms).

6. CONCLUSIONS

The control architecture of an autonomous forklift has been presented. The integration between the motion control developed in theories and the behavior-based control architecture was proposed to produce a fast movement, accident preventive motion, failure recovery action, and high precision motion for autonomous vehicles. A FSM that regulates the the planning and control algorithms was proposed. The proposed control structure integrated multiple sensors, feedback controls, and decision making in a modular fashion for automating a forklift. The effectiveness of the proposed architecture was verified by experimental results of autonomous forklift transporting a pallet from an initial to a desired configuration.

ACKNOWLEDGMENT

This work was supported by the World Class University program granted by the National Research Foundation of Korea under the Ministry of Education, Science and Technology, Korea (grant no. R31-

20004) and the Research and Innovation Program ITB (grant no. 185/I1.C06/PL/2012) granted by the Directorate General of Higher Education under the Ministry of National Education of Indonesia.

7. REFERENCES

Arkin, R. C., 1998, *Behavior-Based Robotics*. Cambridge, MA: MIT Press.

Arkin, R. C., 1992, Behavior-based robot navigation for extended domains. *Adapt. Behav.* **1**, 201–225.

Astolfi, A., 1996, Discontinuous control of nonholonomic systems. *System. Control Lett.* **27**, 37-45.

Belta, C., Isler, V., and Pappas, G. J., 2005, Discrete abstractions for robot motion planning and control in triangular environments. *IEEE Trans. Robot.* **21**, 864-874.

Brockett, R. W., 1983, *Asymptotic stability and feedback stabilization*. Differential geometric control theory. Birkhäuser.

Brooks, R. A., 1986, A robust layered control system for a mobile robot. *IEEE Trans. Robot. Automat.*, **2**, 14–23.

Bui, T. T. Q. and Hong, K.-S., 2010, Sonar-based obstacle avoidance using region partition scheme. *J. Mech. Sci. Technol.* **24**, 365-372.

Bui, T. T. Q. and Hong, K.-S., 2012, Evaluating a color-based active basis model for object recognition. *Comput. Vis. Image Underst.* **116**, 1111-1120.

Conner, D. C., Choset, H., and Rizzi, A. A., 2009, Flow-through policies for hybrid controller synthesis applied to fully actuated systems. *IEEE Trans. Robot.* **25**, 136-146.

Fernandez-Gauna, B., Lopez-Guede, J. M., Zulueta, E., Echegoyen, Z., Grana, M., 2011, Basic results and experiments on robotic multi-agent system for hose deployment and transportation. *Int. J. Artificial Intelligence*. **6**, 183-202.

Gerkey, B. P., and Mataric, M. J., 2002, Sold!: Auction methods for multi-robot coordination. *IEEE Trans. Robot. Autom.* **8**, 758-768.

Haidegger, T., Kovacs, L., Preitl, S., Precup, R.-E., Benyo, B., Benyo, Z., 2011, Controller design solutions for long distance telesurgical applications. *Int. J. Artificial Intelligence*, **6**, 48-71.

Hassanein, O. I., Anavatti, S. G., Ray, T., 2011, Robust position control for two-link manipulator. *Int. J. Artificial Intelligence*. **7**, 347-359.

Hong, K.-S., Tamba, T. A., and Song, J. B., 2008, Mobile robot architecture for reflexive avoidance of moving obstacles. *Adv. Robot.* **22**. 1397-1420.

Joelinato, E., and Wiranto, I., 2011, An application of ant colony optimization, Kalman filter, and artificial neural network for multiple target tracking problems. *Int. J. Artificial Intelligence*. **7**, 384-400.

LaValle, S. M., 2006, *Planning Algorithms*. Cambridge University Press.

Lindemann, S. R., and LaValle, S. M., 2009, Simple and efficient algorithms for computing smooth, collision-free feedback laws over given cell decomposition. *Int. J. Robot. Res.* **28**, 600-621.

Murray, R. M., and Sastry, S. S., 1993, Nonholonomic motion planning: Steering using sinusoids. *IEEE Trans. Automat. Control*, **38**, 700-716.

Nguyen, L. H., Hong, K.-S., and Park, S., 2010, Road-frequency adaptive control for semi-active suspension system. *Int. J. Control Automat. System*. **8**, 1029-1038.

Oreback, A., and Christensen, H. I., 2003, Evaluation of architectures for mobile robotics. *Auton. Robot.* **14**, 33-49.

Samson, C., 1995, Control of chained systems application to path following and time-varying point stabilization of mobile robots. *IEEE Trans. Automat. Control*, **40**, 64-77.

Takemura, Y., and Ishii, K., 2011, Auto color calibration algorithm using neural networks and its application to RoboCup robot vision. *Int. J. Artificial Intelligence*. **7**, 368-383.

Tamba, T. A., Hong, B., and Hong, K.-S., 2009, A path following control of an unmanned autonomous forklift. *Int. J. Control Automat. System*. **7**, 113-122.

Turnip, A., Park, S., and Hong, K.-S., 2010, Sensitivity control of a MR-damper semi-active suspension. *Int. J. Precis. Eng. Manuf.* **11**, 209-218.

Widyotriatmo, A., Hong, B., and Hong, K.-S., 2009, Predictive navigation of an autonomous vehicle with nonholonomic and minimum turning radius constraints. *J. Mech. Sci. Tech.* **23**, 381-388.

Widyotriatmo, A., Hong, K.-S., and Prayudhi, L. H., 2010, Robust stabilization of a wheeled vehicle: Hybrid feedback control design and experimental validation. *J. Mech. Sci. Tech.* **24**, 513-520.

Widyotriatmo, A. and Hong, K.-S., 2011, A navigation function-based control of multiple wheeled vehicles. *IEEE Trans. Indus. Electron.* **58**, 1896-1906.

Widyotriatmo, A., and Hong, K.-S., 2012, Switching algorithm for robust configuration control of a wheeled vehicle. *Control Eng. Practice*. **20**, 315-325.